Results in Physics 7 (2017) 459–469

Contents lists available at ScienceDirect

Results in Physics

journal homepage: www.journals.elsevier.com/results-in-physics

Irreversibility analysis of hydromagnetic flow of couple stress fluid with radiative heat in a channel filled with a porous medium

A.S. Eegunjobi [a,*], O.D. Makinde [b]

[a] Mathematics Department, Namibia University of Science and Technology, Windhoek, Namibia
[b] Faculty of Military Science, Stellenbosch University, Private Bag X2, Saldanha 7395, South Africa

ARTICLE INFO

Article history:
Received 10 November 2016
Accepted 1 January 2017
Available online 7 January 2017

Keywords:
MHD channel flow
Couple stress fluid
Porous medium
Thermal radiation
Entropy generation
Injection/suction

ABSTRACT

Numerical analysis of the intrinsic irreversibility of a mixed convection hydromagnetic flow of an electrically conducting couple stress fluid through upright channel filled with a saturated porous medium and radiative heat transfer was carried out. The thermodynamics first and second laws were employed to examine the problem. We obtained the dimensionless nonlinear differential equations and solves numerically with shooting procedure joined with a fourth order Runge-Kutta-Fehlberg integration scheme. The temperature and velocity obtained, used to analyse the entropy generation rate together with some various physical parameters of the flow. Our results are presented graphically and talk over.

Introduction

In industrial and engineering applications, the conductive couple stress fluids is vital and useful.

The rheological features of such fluids are vital in the extraction of crude oil from petroleum products, aerodynamics heating, electrostatic precipitation, solidification of liquid crystals, cooling of metallic plate in a bath, exotic lubricants, colloidal and suspension solutions. Stoke [1], proposed the micro-continuum theory of couple stress fluid with polar effects and defines the rotational field in terms of the velocity field for setting up the constitutive relationship between the stress and strain rate. Putting applications in consideration, Bujurke and Naduvinamani [2] studied the performance of narrow porous journal bearing lubricated with couple stress fluid. Lin [3] inspected the couple stress fluid model for squeeze film characteristics of finite journal bearings. The analytical solution for Hall and Ion-slip effects on mixed convection flow of couple stress fluid between parallel disks was conveyed by Srinivasacharya and Kaladhar [4]. Meanwhile, conductive couple stress fluids can support magnetic fields. The forces that act on the fluid is due to the presence of magnetic, thereby possibly altering the geometry and strength of the magnetic fields themselves. The relative strength of the advecting motions in the fluid which form the central point of magnetohydrodynamics (MHD) theory is the key issue for a particular conducting fluid. The heat transfer to magnetohydrodynamics non-Newtonian couple stress pulsatile flow between two parallel porous plates was studied by Adesanya and Makinde [5]. Muthuraj et al. [6] investigated numerically the combined effects of heat and mass transfer on MHD flow of a couple stress fluid in a horizontal wavy walled channel filled with a porous medium in the presence viscous dissipation. The hypothetical studied of MHD oscillatory slip flow and heat transfer in a channel filled with porous media was analysed by Adesanya and Makinde [7]. When the flow systems operate at high temperature, there exists thermal radiation effect. Heat transfer by concurrent radiation and convection are frequently encountered in numerous technological problems including combustion, furnace design, the design of high temperature gas cooled in nuclear reactors, nuclear reactor safety, fluidized bed heat exchanger, solar fans, solar collectors, natural convection in cavities, and many others. The combined radiation and mixed convection from a vertical wall with injection/suction in a non- Darcy porous medium was studied by Murthy et al. [8]. The impact of thermal radiation on free convection flow through a porous medium was investigated by Raptis [9]. Makinde and Animasaun [10] numerically considered the effects of nonlinear thermal radiation on MHD bioconvection of conducting nanofluid with quartic autocatalysis chemical reaction past an upper surface of a paraboloid of revolution.

Meanwhile, fluid flow and heat transfer processes are basically irreversible due to entropy production. Bejan [11] announced the concept of entropy generation analysis due to fluid flow and heat

* Corresponding author.
E-mail address: samdet1@yahoo.com (A.S. Eegunjobi).

http://dx.doi.org/10.1016/j.rinp.2017.01.002
2211-3797/

transfer as an effective tool to evaluate the performance of engineering devices. After his pioneering work, several researchers have analysed the fluid flow irreversibility problems under various physical situation [12–15]. Makinde and Eegunjobi [16] investigated the entropy generation rate in a couple stress fluid flows through a vertical channel filled with saturated porous media. Tasnim et al. [17] studied the effects of magnetic field on entropy generation rate in an isothermal porous two dimensional channel.

To the best of our knowledge, the mutual effects of magnetic field, thermal radiation, buoyancy force and convective heat transfer on entropy generation in a mixed convective flow of an electrically conducting couple stress fluid through a vertical channel packed with a saturated porous medium has not been reported yet in the literature. Our main objective is to tackle this problem theoretically by considering the inherent irreversibility in a mixed convection hydromagnetic flow of an electrically conducting couple stress fluid through a vertical channel packed with a saturated porous medium with radiative heat transfer. In the subsequent sections, the problem is formulated, we dimensionless the equations and solved. Relevant results are presented graphically and discussed.

Mathematical formulation

An electrically conducting incompressible, radiating couple stress fluid of an hydromagnetic steady flow in a vertical position channel, filled with a saturated homogeneous porous medium together with permeable walls as shown in Fig. 1 was considered. We assumed that the left wall (where fluid injection takes place) is upheld at a uniform temperature while the convective heat exchange with the surrounding fluid occurs at the right wall (where fluid suction occurs). The flow occurs in the direction of x-axis and the y-axis is taken perpendicular to it. The influences of an external, transversely applied, uniform magnetic fields of strength B_0 are on the flow field. The effect of magnetic Reynolds number and the induced electric field are assumed to be minor and insignificant. We denoted the distance between two permeable walls of the channel by a and the length by L. we put into consideration the thermal radiation that takes place during flow process in the channel as well as the velocity slip at the right.

Using Brinkman–Forchheimer flow model, the governing equations are obtained from the balance of linear momentum, energy and volumetric entropy generation rate equations as [6,12–14,16]:

$$-V\frac{du}{dy} = -\frac{1}{\rho}\frac{\partial P}{\partial x} + \upsilon\frac{d^2u}{dy^2} - \frac{\delta}{\rho}\frac{d^4u}{dy^4} - \frac{\sigma B_0^2 u}{\rho} - \frac{\upsilon u}{k_1} - \frac{cu^2}{\rho\sqrt{k_1}} + g\beta(T - T_w), \tag{1}$$

$$-V\frac{dT}{dy} = \frac{k}{\rho c_p}\frac{d^2T}{dy^2} + \frac{\upsilon}{c_p}\left(\frac{du}{dy}\right)^2 + \frac{\delta}{\rho c_p}\left(\frac{d^2u}{dy^2}\right)^2 - \frac{1}{\rho c_p}\frac{\partial q_r}{\partial y} + \frac{\sigma B_0^2 u^2}{\rho c_p} + \frac{\upsilon u^2}{k_1 c_p} + \frac{cu^3}{\rho c_p\sqrt{k_1}}, \tag{2}$$

$$E_G = \frac{k}{T_w^2}\left(1 + \frac{16\sigma^* T^3}{3k^* k}\right)\left(\frac{dT}{dy}\right)^2 + \frac{\mu}{T_w}\left(\frac{du}{dy}\right)^2 + \frac{\delta}{T_w}\left(\frac{d^2u}{dy^2}\right)^2 + \frac{\sigma B_0^2 u^2}{T_w} + \frac{\mu u^2}{T_w k_1} + \frac{cu^3}{T_w\sqrt{k_1}}. \tag{3}$$

The suitable boundary conditions for the fluid velocity and temperature are given as

$$u = \frac{d^2u}{dy^2} = 0, T = T_w = 0, \text{ at } y = 0, \tag{4}$$

$$u = \frac{d^2u}{dy^2} = 0, -k\frac{dT}{dy} = h(T - T_w), \text{ at } y = a, \tag{5}$$

here u is the axial velocity, h represents wall heat transfer coefficient, μ stands for the dynamic viscosity, ρ is the fluid density, E_G is the entropy generation rate, T is the fluid temperature, c_p is specific heat at constant pressure, σ is the electrical conductivity, g is the gravitational acceleration, δ is the fluid particle size effect due to couple stresses, V is the wall injection/suction velocity, T_w is the channel left wall temperature, β is the thermal expansion coefficient, k is the thermal conductivity of the fluid, $k_1$is the porous media permeability, c is the empirical constant in the second order (porous inertia) resistance such that $c = 0$ corresponds to the Darcy law. By assuming Rosseland approximation [8–10] the radiative heat flux is taken as

$$q_r = -\frac{4\sigma^*}{3k^*}\frac{\partial T^4}{\partial y} = -\frac{16\sigma^* T^3}{3k^*}\frac{\partial T}{\partial y}, \tag{6}$$

where σ^* is the Stefan–Boltzmann constant and $k*$ is the mean absorption coefficient. We present the dimensionless variables and parameters as follows:

$$\eta = \frac{y}{a}, X = \frac{x}{a}, \theta = \frac{T - T_w}{T_w}, \upsilon = \frac{\mu}{\rho}, w = \frac{ua}{\upsilon}, \Pr = \frac{\mu c_p}{k}, Ec = \frac{\upsilon^2}{c_p T_w a^2},$$
$$\lambda = \frac{\delta}{\rho\upsilon a^2}, A = -\frac{\partial\bar{P}}{\partial X}, M = \frac{\sigma B_0^2 a^2}{\rho\upsilon}, Nr = \frac{16\sigma^* T_w^3}{3k^* k}, Ns = \frac{E_G a^2}{k}, \tag{7}$$
$$S_1 = \frac{a^2}{k_1}, S_2 = \frac{ca}{\rho\sqrt{k_1}}, \mathrm{Re} = \frac{Va}{\upsilon}, \bar{P} = \frac{a^2 p}{\rho\upsilon^2}, Gr = \frac{g\beta T_w a^3}{\upsilon^2}, Bi = \frac{ah}{k}.$$

Replacing Eq. (7) into Eqs. (1)–(6), we get,

$$\frac{d^2w}{d\eta^2} - \lambda\frac{d^4w}{d\eta^4} + \mathrm{Re}\frac{dw}{d\eta} - (M + S_1)w - S_2 w^2 + Gr\theta + A = 0, \tag{8}$$

$$\left[1 + Nr(\theta + 1)^3\right]\frac{d^2\theta}{d\eta^2} + 3Nr(\theta + 1)^2\left(\frac{d\theta}{d\eta}\right)^2 + \mathrm{PrRe}\frac{d\theta}{d\eta} + \mathrm{PrEc}\left[\left(\frac{dw}{d\eta}\right)^2 + \lambda\left(\frac{d^2w}{d\eta^2}\right)^2 + (M + S_1)w^2 + S_2 w^3\right] = 0, \tag{9}$$

$$Ns = \left[1 + Nr(\theta + 1)^3\right]\left(\frac{d\theta}{d\eta}\right)^2 + \mathrm{PrEc}\left[\left(\frac{dw}{d\eta}\right)^2 + \lambda\left(\frac{d^2w}{d\eta^2}\right)^2 + (M + S_1)w^2 + S_2 w^3\right], \tag{10}$$

with

$$w = \frac{d^2w}{d\eta^2} = 0, \theta = 0, \text{ at } \eta = 0, \tag{11}$$

$$w = \frac{d^2w}{d\eta^2} = 0, \frac{d\theta}{d\eta} = -Bi\theta, \text{ at } \eta = 1, \tag{12}$$

where Pr is the Prandtl number, Re is the injection/suction Reynolds number, Gr is the Grashof number, Bi is the Biot number, λ is the couple stress parameter, Ec is the Eckert number, A is pressure gradient, S_1 is the porous medium shape factor parameter, S_2 is the second order porous medium resistance parameter, M is the magnetic field parameter, Br (=$EcPr$) is the Brinkmann number and Nr is the radiation parameter. Other quantities of concern are the skin friction coefficients (C_f), Nusselt number (Nu) and the Bejan number (Be) which are given as

$$C_f = \frac{\rho h^2\tau_w}{\mu^2} = \left.\frac{dw}{d\eta}\right|_{\eta=0,1},$$
$$Nu = -\frac{hq_m}{kT_w} = -\left[1 + Nr(\theta + 1)^3\right]\left.\frac{d\theta}{d\eta}\right|_{\eta=0,1}, Be = \frac{N_1}{Ns} = \frac{1}{1 + \phi}, \tag{13}$$

where

$$\tau_w = \mu\frac{\partial u}{\partial y}, q_m = -k\left(1+\frac{16\sigma^* T^3}{3kk^*}\right)\frac{\partial T}{\partial y},$$
$$N_1 = \left[1+Nr(\theta+1)^3\right]\left(\frac{d\theta}{d\eta}\right)^2, \phi = \frac{N_2}{N_1}, \tag{14}$$

$$N_2 = \mathrm{Pr}Ec\left[\left(\frac{dw}{d\eta}\right)^2 + \lambda\left(\frac{d^2w}{d\eta^2}\right)^2 + (M+S_1)w^2 + S_2w^3\right] \tag{15}$$

The sign N_1 represents thermodynamic irreversibility due to thermal radiation absorption and heat transfer while N_2 denote the combined effects of fluid friction, magnetic field and porous media irreversibility [11,18]. If $Be \in (0.5, 1)$ then the effects of thermodynamics irreversibility due to thermal radiation absorption and heat transfer dominate the flow system. But $0 \leqslant \mathrm{Be} < 0.5$ corresponds to the dominant effects of fluid friction, magnetic field and porous media irreversibilities. $Be = 0.5$ means that both N_1 and N_2 contribute equally to the entropy generation rate and ϕ is the irreversibility ratio. We solved the model Eqs. (8)–(12) using a shooting method coupled with the Runge-Kutta-Fehlberg integration scheme numerically [19].

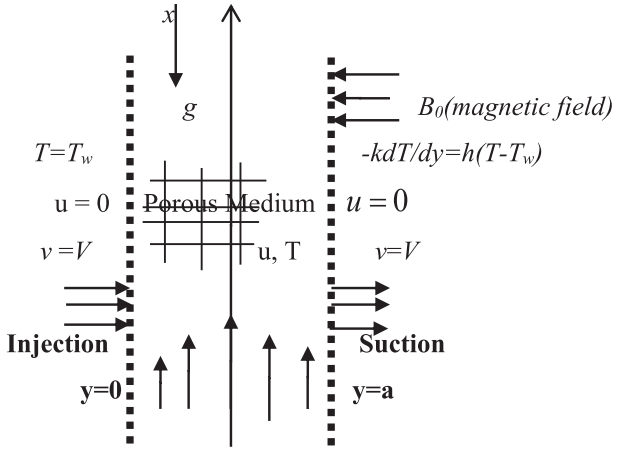

Fig. 1. Physical model of the problem.

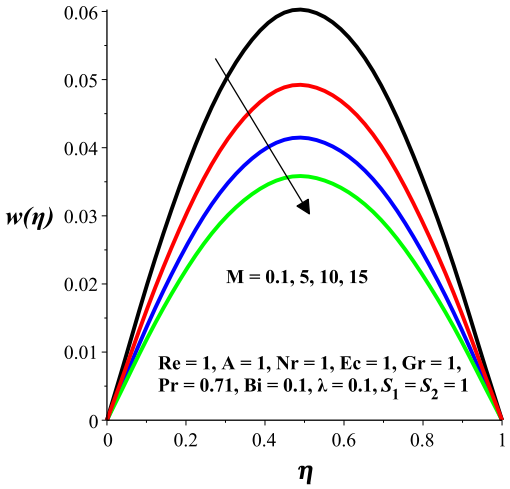

Fig. 2. Velocity profiles with increasing Gr.

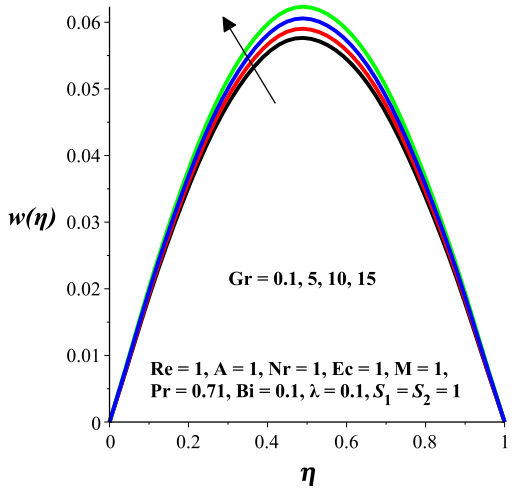

Fig. 3. Velocity profiles with increasing Gr.

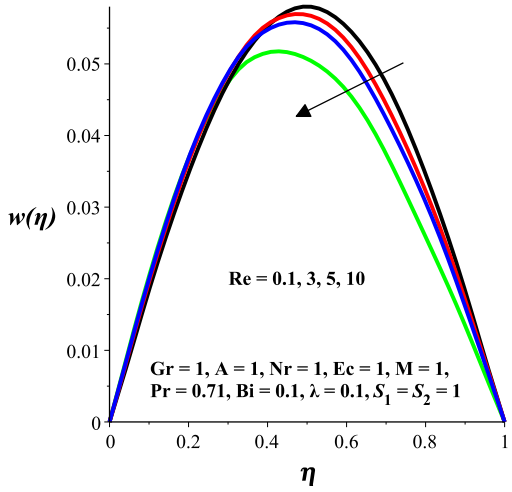

Fig. 4. Velocity profiles with increasing Re.

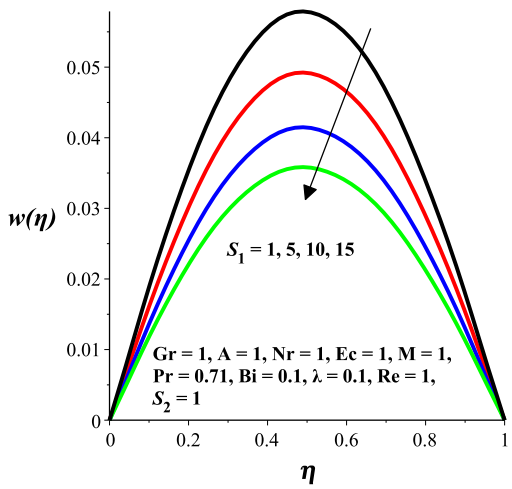

Fig. 5. Velocity profiles with increasing S_1.

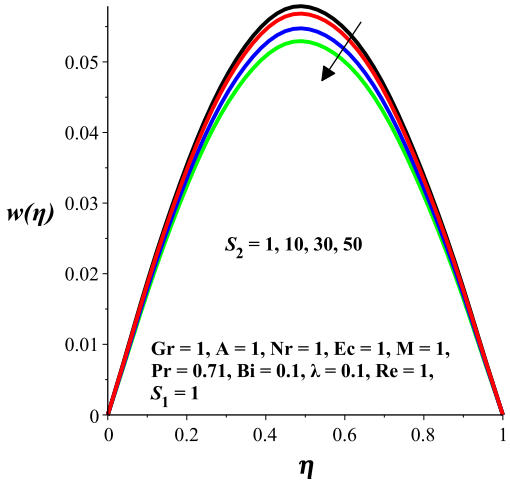

Fig. 6. Velocity profiles with increasing S_2.

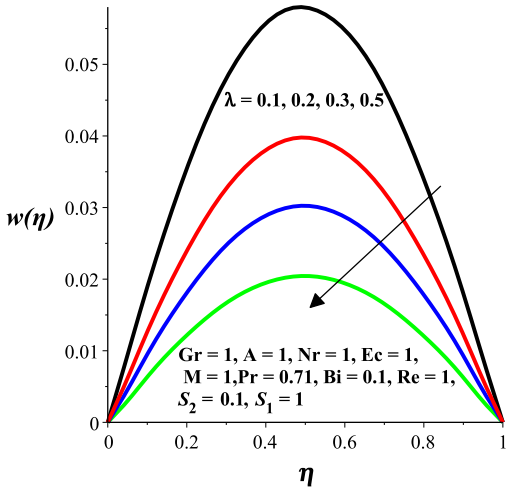

Fig. 7. Velocity profiles with increasing λ.

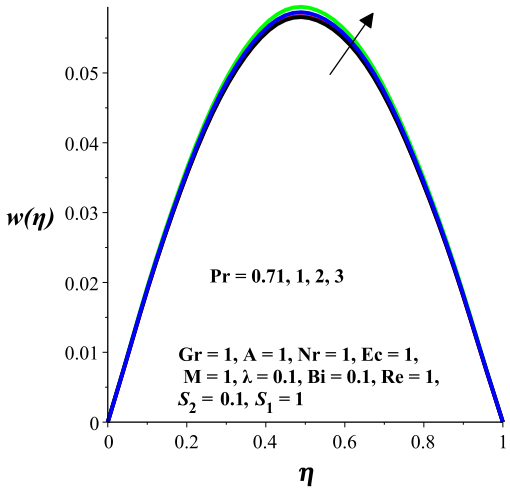

Fig. 8. Velocity profiles with increasing Pr.

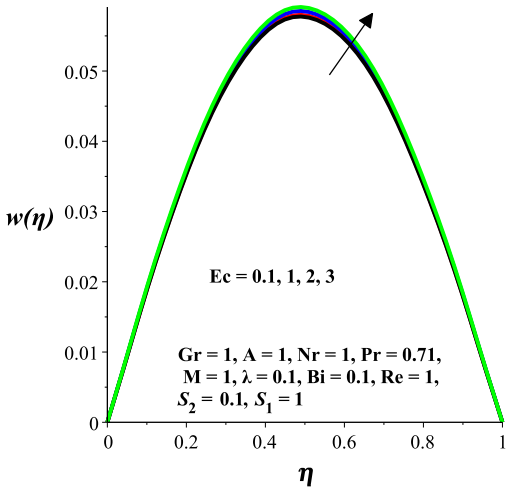

Fig. 9. Velocity profiles with increasing Ec.

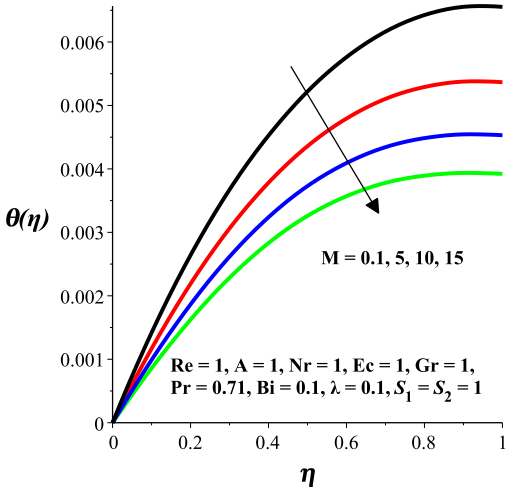

Fig. 10. Temperature profiles with increasing M.

Results and discussion

For better understanding of the flow and thermal systems, we assigned some arbitrary values to various thermophysical parameters controlling the flow and thermal systems and carried out the numerical solution for the representative velocity field, temperature field, skin friction, Nusselt number, entropy generation rate and Bejan number as shown in Figs. 2-45.

Velocity profiles

Figs. 2–9 show the impact of varying parameters on the couple stress fluid velocity profiles. In general, the velocity profiles are parabolic in nature, with zero value at the walls due to no slip condition. It is noticed that velocity profiles attained its maximum value around the channel centreline region. An increase in magnetic field intensity (M) suppresses the fluid velocity as shown in Fig. 2. This may be ascribed to the existence of Lorentz force which tends to retard the fluid motion. Fig. 3 shows the impact of Grashof number (Gr) on the velocity profile. It can be seen in this figure that the velocity flow profile accelerates with increasing Gr due to thermal buoyancy effect. Fig. 4 gives a picture of the effect of Reynolds (Injection/Suction) (Re) on the velocity profile. From Fig. 4, it can be

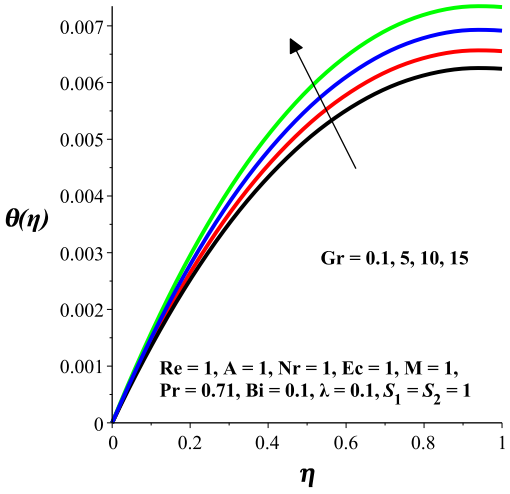

Fig. 11. Temperature profiles with increasing Gr.

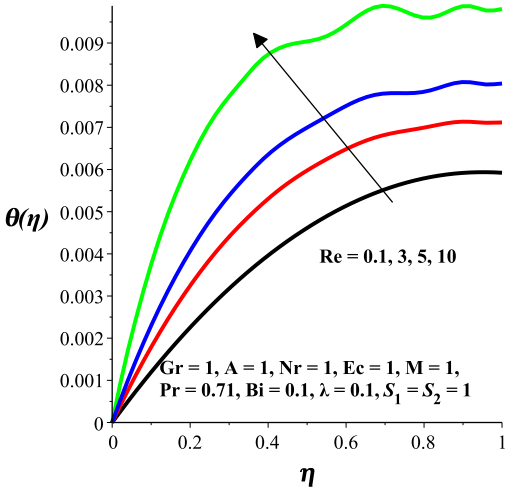

Fig. 12. Temperature profiles with increasing Re.

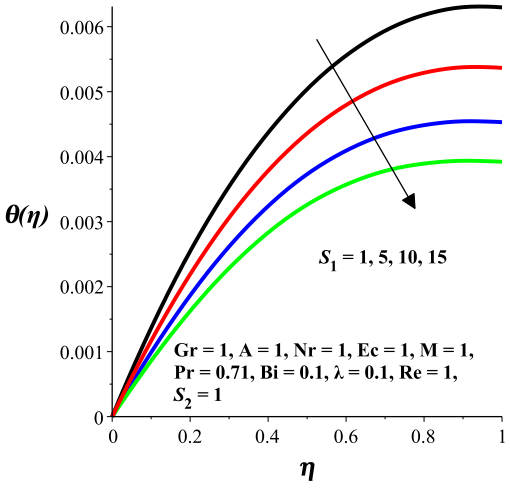

Fig. 13. Temperature profiles with increasing S_1.

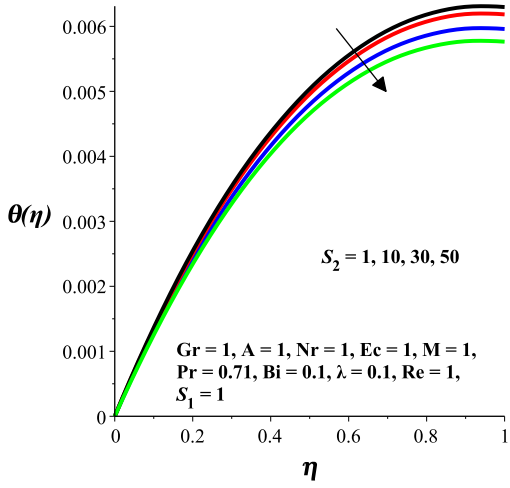

Fig. 14. Temperature profiles with increasing S_2.

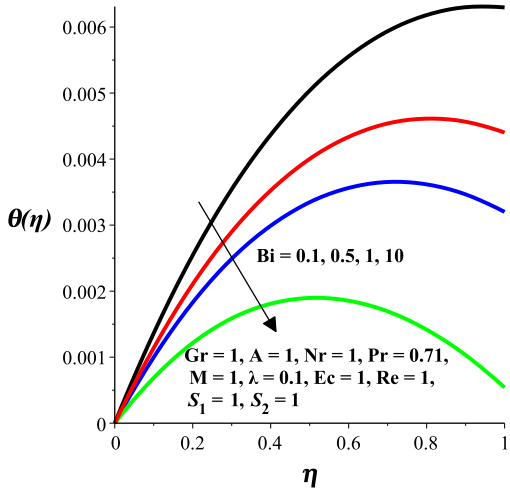

Fig. 15. Temperature profiles with increasing **Bi**.

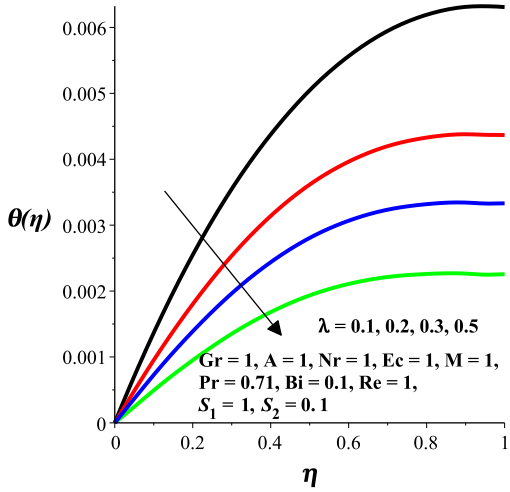

Fig. 16. Temperature profiles with increasing λ.

seen that as Re is increasing, there exit a cross flow with increasing injection at the left wall and increasing suction at the right wall. Also, velocity profile tends to decrease but skewed towards the right wall. The effect of porous medium parameters S_1 and S_2 is to subdue the flow as shown in Figs. 5 and 6, because of the dampening effect of Darcy resistance. Fig. 7 depicts the effects of couple

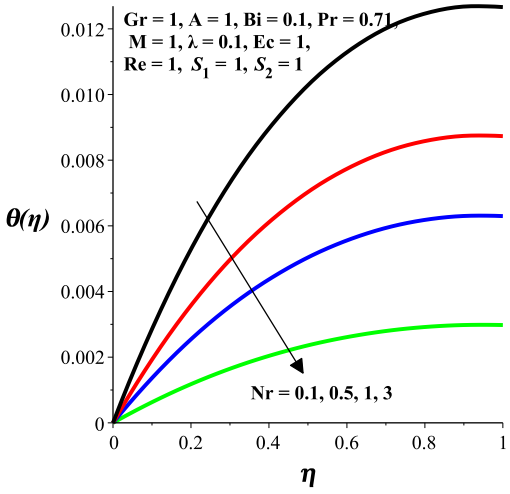

Fig. 17. Temperature profiles with increasing Nr.

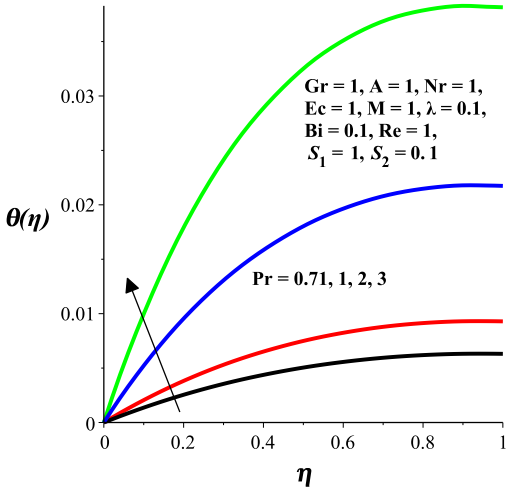

Fig. 18. Temperature profiles with increasing Pr.

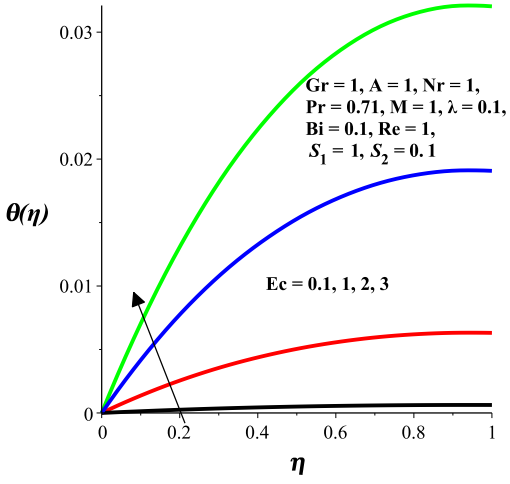

Fig. 19. Temperature profiles with increasing Ec.

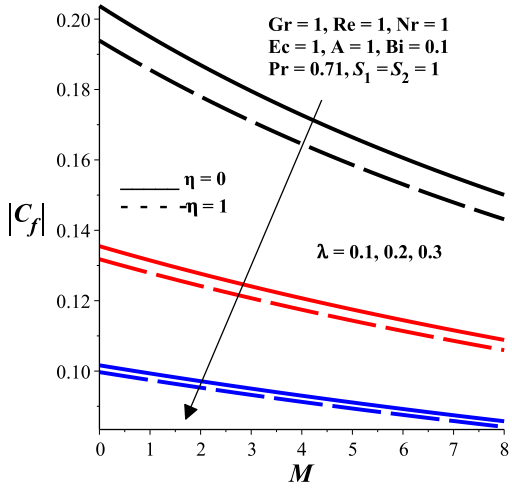

Fig. 20. Skin friction with increasing M and λ.

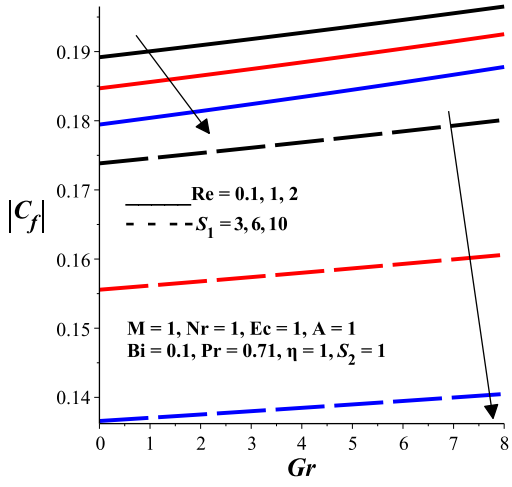

Fig. 21. Skin friction with increasing Re, Gr and S_1.

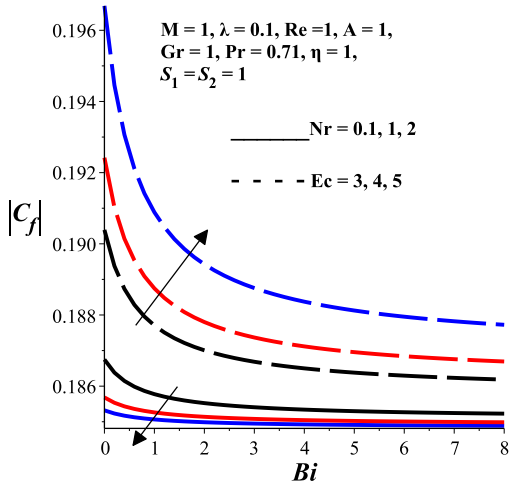

Fig. 22. Skin friction with increasing Bi, Nr and Ec.

stress parameter λ on the velocity profile. Here, the velocity profile is suppressed as the couple stress parameter λ increases. It is noteworthy that, as λ tends to zero, the fluid becomes newtonian fluid.

The influences of Prandtl number (Pr) and Eckert (Ec) number are shown in Figs. 8 and 9. From these figures, it can be seen that as Pr and Ec increase, the fluid velocity also increases due to a rise in viscous heating.

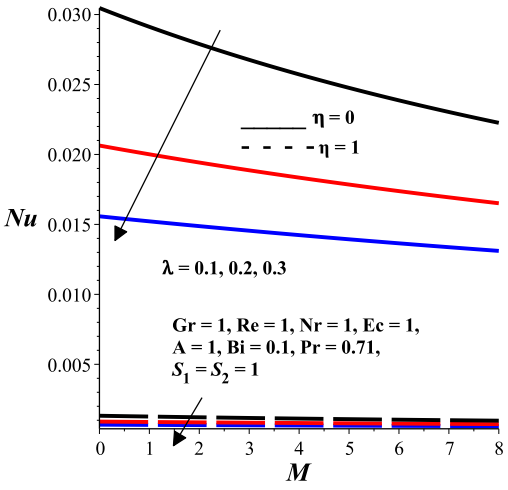

Fig. 23. Nusselt number with increasing M and λ.

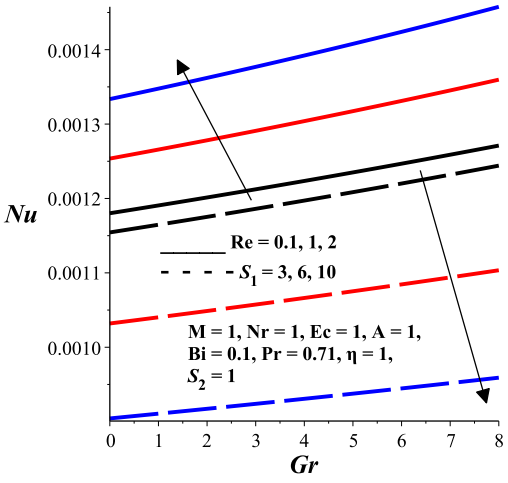

Fig. 24. Nusselt number with increasing Re, Gr and S_1.

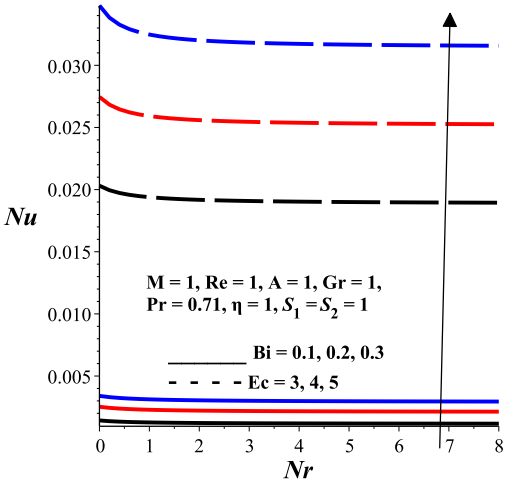

Fig. 25. Nusselt number with increasing Bi, Ec and Nr.

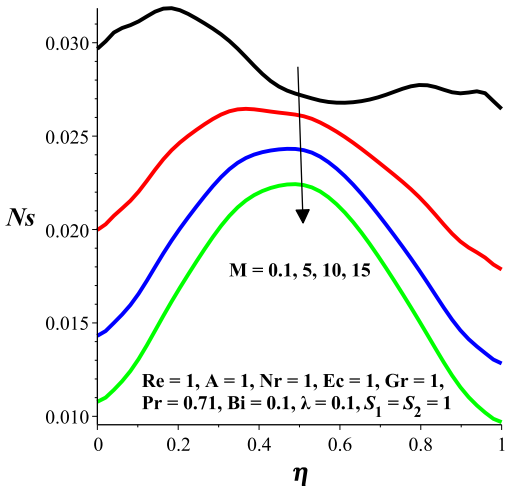

Fig. 26. Entropy generation rate with increasing M.

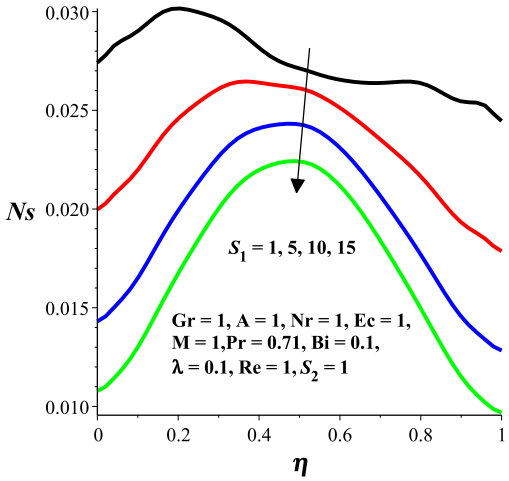

Fig. 27. Entropy generation rate with increasing S_1.

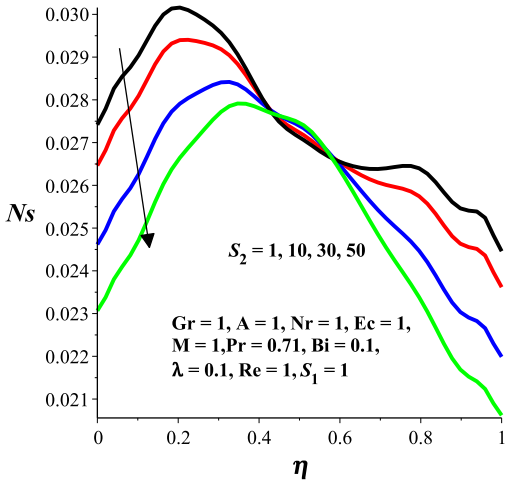

Fig. 28. Entropy generation rate with increasing S_2.

Temperature profiles

The graphical illustrations of the effects of various parameters on the temperature profiles are presented in Figs. 10–19. Generally, the fluid temperature attained its lowest value at the left wall. Thereafter, it starts increasing gradually to the pick value within, then decreases to the right wall due to convective heat loss to the ambient. In Fig. 10, it is detected that an increase in magnetic

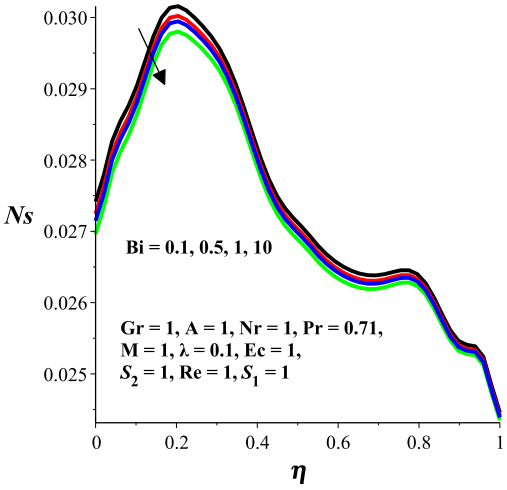

Fig. 29. Entropy generation rate with increasing Bi.

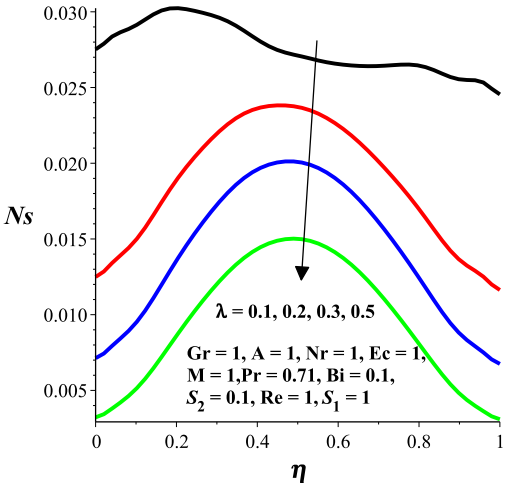

Fig. 30. Entropy generation rate with increasing λ.

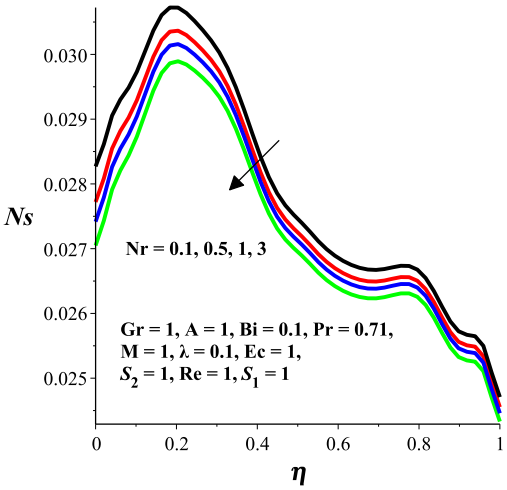

Fig. 31. Entropy generation rate with increasing Nr.

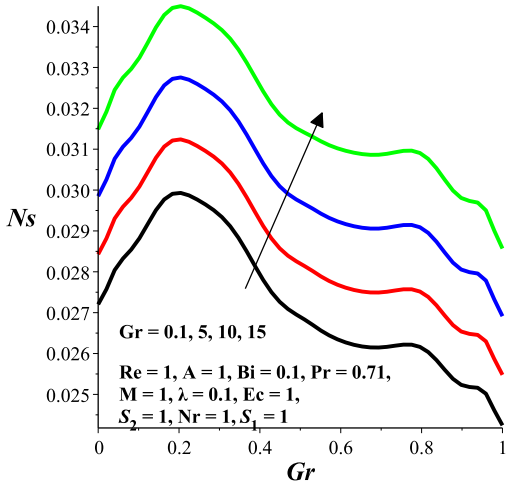

Fig. 32. Entropy generation rate with increasing Gr.

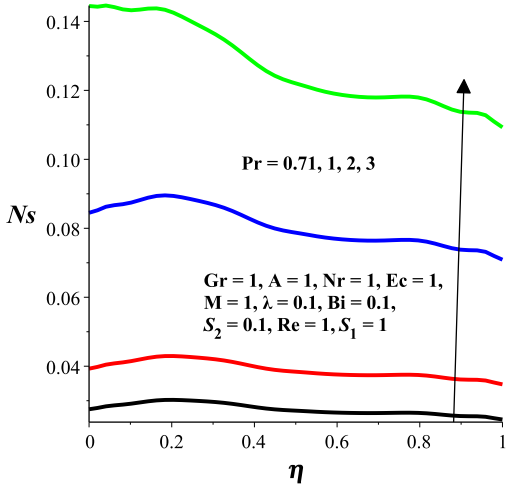

Fig. 33. Entropy generation rate with increasing Pr.

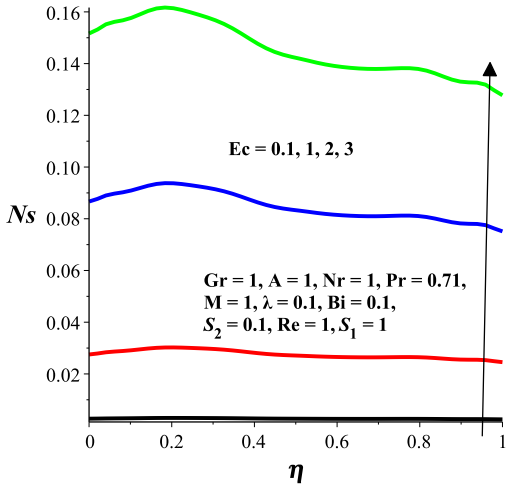

Fig. 34. Entropy generation rate with increasing Ec.

field intensity (M) diminishes the couple stress fluid temperature. This may be attributed to the combined effects of a decrease in the velocity gradient with an increasing M and the convective heat loss to the ambient. Figs. 11 and 12 depict the effect of increasing Gr and Re on the temperature profiles. Interestingly, the fluid temperature upsurges with increasing Grashof number (Gr) due to ther-

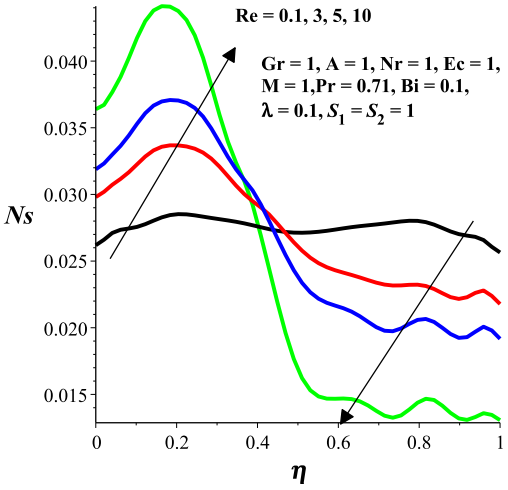

Fig. 35. Entropy generation rate with increasing Re.

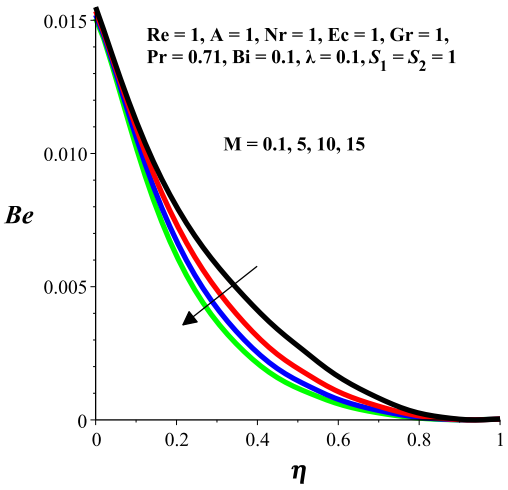

Fig. 36. Bejan number with increasing M.

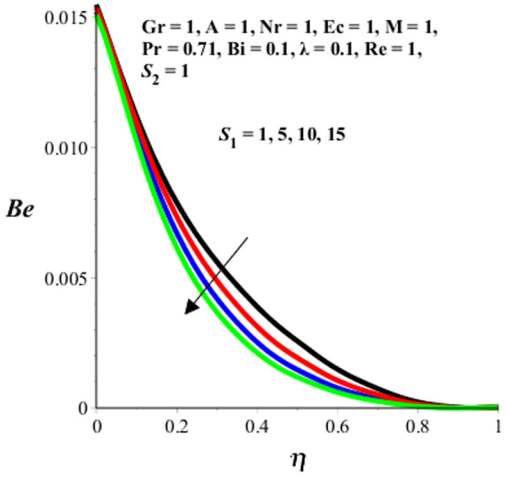

Fig. 37. Bejan number with increasing S_1.

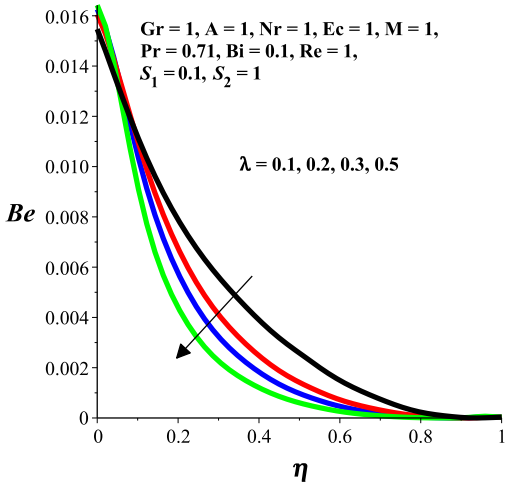

Fig. 38. Bejan number with increasing λ.

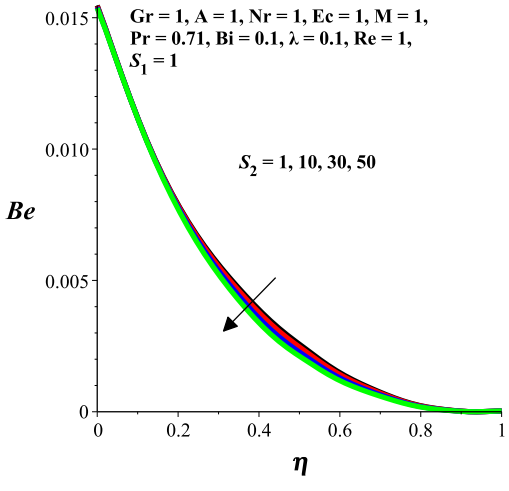

Fig. 39. Bejan number with increasing S_2.

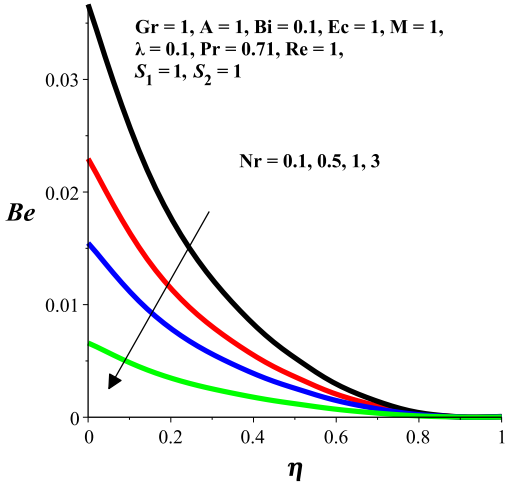

Fig. 40. Bejan number with increasing Nr.

mal buoyancy effect and injection/suction parameter (Re). It is can be seen as Re increases, both the fluid injection into the channel at the left permeable wall and the fluid suction out of the channel at the right permeable wall also rises. Consequently, the velocity gradient across the channel also increases, leading to a rise in the fluid temperature. In Figs. 13 and 14, it is observed that the fluid tem-

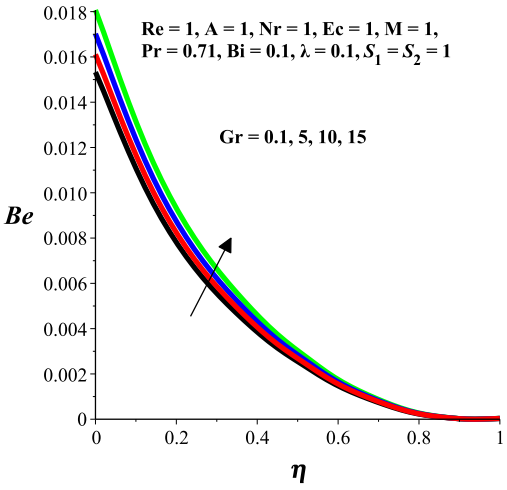

Fig. 41. Bejan number with increasing Gr.

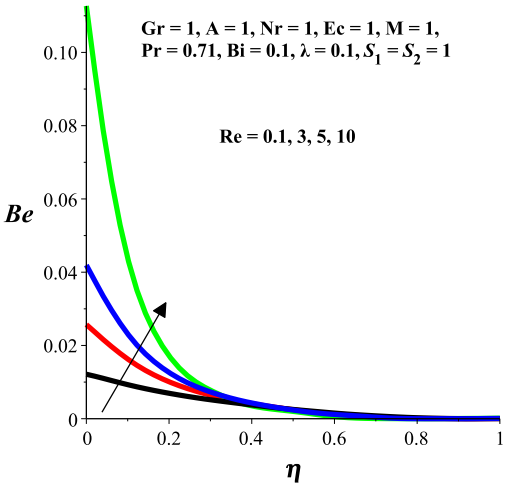

Fig. 42. Bejan number with increasing Re.

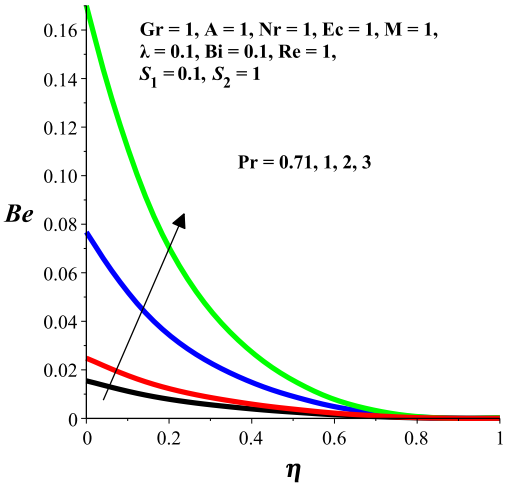

Fig. 43. Bejan number with increasing Pr.

perature decreases with increasing values of porous medium parameters S_1 and S_2. As these parameters increase, the porous medium permeability decreases, leading to a decrease in the fluid

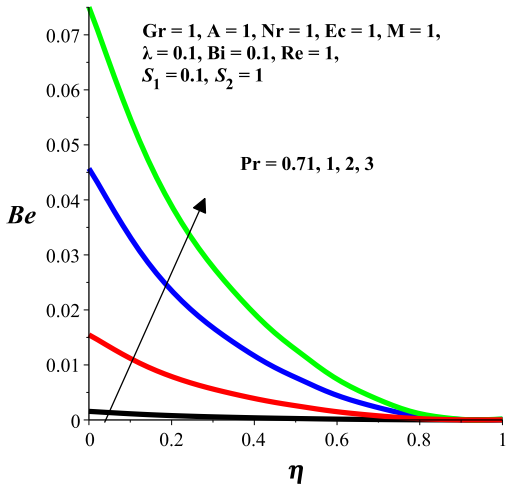

Fig. 44. Bejan number with increasing Ec.

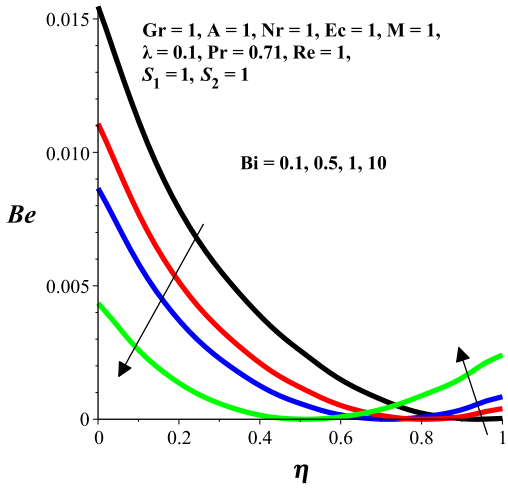

Fig. 45. Bejan number with increasing Bi.

velocity gradient and temperature. The fluid temperature decreases with an increase in Biot number (*Bi*) as shown in Fig. 15. This is expected due to convective cooling. As *Bi* increases, the rate of convective heat loss to the ambient from the right wall of the channel increases, leading to a fall in the fluid temperature. An increase in the couple stress parameter (λ) results to a decrease in the fluid temperature as shown in Fig. 16. The effect of radiation absorption parameter (Nr) on the temperature profile is illustrated in Fig. 17. Here, we see that the fluid temperature decline with an increase in Nr. We note that the fluid temperature increases with an increase in the parameter values of Pr and *Ec* as shown in Figs. 18 and 19. This is because both the Prandtl number (Pr) and Eckert number (Ec) enhanced viscous heating within the flow.

Skin friction and Nusselt number

The effects of thermophysical parameters on the wall shear stress and wall heat flux are displayed in Figs. 20–25. Interestingly, it is observed in Figs. 20–22 that the skin friction at both walls increases with an increase in parameter values of Gr and Ec, but decreases with an increase in the parameter values of Re, Bi, M, Nr, S_1 and λ. This can be ascribed to the fact that as Gr and Ec increases, the velocity gradient at the channel walls increases, while as Re, Bi, M, Nr, S_1 and λ increases, the velocity gradient

decreases, consequently the skin friction increases or decreases. Meanwhile, the Nusselt number increases with rise in the parameter values of Re, Bi, Gr and Ec but decreases with an increase in the parameter values of M, Nr, S_1 and λ as depicted in Figs. 23–25. These increase or decrease in the Nusselt number can be attributed to a rise or fall in the temperature gradient at the channel walls.

Entropy generation rate

The effects of various thermophysical parameters on entropy production within the channel are displayed Figs. 26–35. It is notable that entropy generation rate is higher at the left wall than the right wall. This may be attributed to the effects of convective cooling at the right wall. Meanwhile, entropy production attained its pick value within the channel. Figs. 26–34 show that entropy production within the channel flow decreases with increasing parameter values of M, S_1, S_2, Bi, λ and Nr but increases with an increase in the parameter values of Gr, Pr and Ec. This decrease and increase in the entropy production with parameters variation can be attributed to the effects of the combined decrease or increase in both velocity and temperature gradients together with the Joule heating within the flow system as reflected in Eq. (10). Moreover, it is interesting to note that the entropy production at the left wall region increases due to an increase in fluid injection, while entropy production at the right wall region decreases due to the increasing rate of fluid suction as shown in Fig. 35.

Bejan number

Figs. 36–45 illustrate the influences thermophysical parameters have on the Bejan number profile. Generally, at the left wall, the Bejan number is at its highest then decreases gradually to its lowest value at the right wall. This is due to the fact that the activity of thermodynamic irreversibility due to heat transfer is paramount at the left wall, while the irreversibility due to fluid friction, magnetic field and porous medium dominate at the right wall. Moreover, an increase in the parameter values of M, S_1, S_2, Nr and λ decreases the Bejan number and increases the dominant tendency of fluid friction, magnetic field and porous media irreversibility as shown in Figs. 36–40. In Fig. 41–44, we observed that the Bejan number increases with an increase in the parameter values on Gr, Re, Pr and Ec. This implies that as these parameters increase, the activity of thermodynamic irreversibility due to heat transfer increases. Fig. 45 shows that an increase in convective cooling (Bi) decreases the Bejan number across the channel but increases the Bejan number near the right wall region.

Conclusion

The inherent irreversibility in a mixed convection hydromagnetic flow of an electrically conducting couple stress fluid through a vertical channel packed with a saturated porous medium with radiative heat transfer has been carried out. We solved the dimensionless governing differential equations numerically using a shooting method together with Runge-Kutta-Fehlberg integration techniques. Our results can be summarized as follows:

- Increase in M, Re, S_1, S_2 and λ decreases the velocity profile, while increase in Pr, Ec and Gr increases the velocity profile.
- Increase in M, S_1, S_2, Bi, λ and Nr decreases the temperature profile, while increase in Gr, Re, Pr and Ec increases the temperature profile.
- The skin friction decreases with an increase in Re, Bi, M, Nr, S_1 and λ, while it increases with an increase in Gr and Ec.
- The Nusselt number increases with an increase in Re, Bi, Gr and Ec, while it decreases with an increase in M, Nr, S_1 and λ.
- The entropy generation rate decreases with an increase in M, S_1, S2, Bi, λ and Nr, while it increases with an increase in of Gr, Pr and Ec.
- The Bejan number decreases with an increase in M, S_1, S_2, λ and Nr, while it increases with an increase in Gr, Re, Pr and Ec.

References

[1] Stokes VK. Couple stresses in fluid. Phys Fluids 1966;9:1709–15.
[2] Bujurke NM, Naduvinamani NB. On the performance of narrow porous journal bearing lubricated with couple stress fluid. Acta Mech 1991;86(1–4):179–91.
[3] Lin J. Squeeze film characteristics of finite journal bearings: couple stress fluid model. Tribol Int 1998;31(4):201–7.
[4] Srinivasacharya D, Kaladhar K. Analytical solution for Hall and Ion-slip effects on mixed convection flow of couple stress fluid between parallel disks. Math Comput Modell 2013;57:2494–509.
[5] Adesanya SO, Makinde OD. Heat transfer to magnetohydrodynamic non-Newtonian couple stress pulsatile flow between two parallel porous plates. Z Naturforsch 2012;67:647–56.
[6] Muthuraj RS, Srinivas S, Selvi RK. Heat and mass transfer effects on MHD flow of a couple-stress fluid in a horizontal wavy channel with viscous dissipation and porous medium. Heat Transfer-Asian Res 2013;42(5):403–21.
[7] Adesanya SO, Makinde OD. MHD oscillatory slip flow and heat transfer in a channel filled with porous media. UPB Sci Bull, Ser A 2014;1:197–204.
[8] Murthy PVSN, Mukherjee S, Srinivascharya D, Krishna PVSSSR. Combined radiation and mixed convection from a vertical wall with suction/injection in a non-Darcy porous medium. Acta Mech 2004;168:145–56.
[9] Raptis A. Radiation and free convection flow through a porous medium. Int Commun Heat Mass Transfer 2009;25:289–95.
[10] Makinde OD, Animasaun IL. Bioconvection in MHD nanofluid flow with nonlinear thermal radiation and quartic autocatalysis chemical reaction past an upper surface of a paraboloid of revolution. Int J Therm Sci 2016;109:159–71.
[11] Bejan A. Entropy generation through heat and fluid flow. New York: Wiley; 1982.
[12] Adesanya SO, Makinde OD. Entropy generation in couple stress fluid flow through porous channel with fluid slippage. Int J Exergy 2014;15(3):344–62.
[13] Adesanya SO, Makinde OD. Irreversibility analysis in a couple stress film flow along an inclined heated plate with adiabatic free surface. Phys A 2015;432:222–9.
[14] Adesanya SO, Makinde OD. Effects of couple stresses on entropy generation rate in a porous channel with convective heating. Comput Appl Math 2015;34:293–307.
[15] Chauhan DS, Kumar V. Heat transfer and entropy generation during compressible fluid flow in a channel partially filled with porous medium. Int J Energy Technol 2011;3:1–10.
[16] Makinde OD, Eegunjobi AS. Entropy generation in a couple stress fluid flow through a vertical channel filled with saturated porous media. Entropy 2013;15:4589–606.
[17] Tasnim SM, Mahmud S, Mamum MAH. Entropy generation in a porous channel with hydromagetic effect. Int. J. Exergy 2002;3:300–8.
[18] Wood LC. Thermodynamics of fluid systems. Oxford, UK: Oxford University Press; 1975.
[19] Cebeci T, Bradshaw P. Physical and computational aspects of convective heat transfer. New York, NY, USA: Springer; 1988.